JACS
JOURNAL OF THE AMERICAN CHEMICAL SOCIETY
Communication
pubs.acs.org/JACS

Atomically Thick Bismuth Selenide Freestanding Single Layers Achieving Enhanced Thermoelectric Energy Harvesting

Yongfu Sun,[†] Hao Cheng,[‡] Shan Gao,[†] Qinghua Liu,[‡] Zhihu Sun,[‡] Chong Xiao,[†] Changzheng Wu,[†] Shiqiang Wei,[‡,*] and Yi Xie*[,†]

[†]Hefei National Laboratory for Physical Sciences at the Microscale, University of Science and Technology of China, Hefei, Anhui 230026, P. R. China

[‡]National Synchrotron Radiation Laboratory, University of Science and Technology of China, Hefei, Anhui 230029, P. R. China

Supporting Information

ABSTRACT: Thermoelectric materials can realize significant energy savings by generating electricity from untapped waste heat. However, the coupling of the thermoelectric parameters unfortunately limits their efficiency and practical applications. Here, a single-layer-based (SLB) composite fabricated from atomically thick single layers was proposed to optimize the thermoelectric parameters fully. Freestanding five-atom-thick Bi_2Se_3 single layers were first synthesized via a scalable interaction/exfoliation strategy. As revealed by X-ray absorption fine structure spectroscopy and first-principles calculations, surface distortion gives them excellent structural stability and a much increased density of states, resulting in a 2-fold higher electrical conductivity relative to the bulk material. Also, the surface disorder and numerous interfaces in the Bi_2Se_3 SLB composite allow for effective phonon scattering and decreased thermal conductivity, while the 2D electron gas and energy filtering effect increase the Seebeck coefficient, resulting in an 8-fold higher figure of merit (ZT) relative to the bulk material. This work develops a facile strategy for synthesizing atomically thick single layers and demonstrates their superior ability to optimize the thermoelectric energy harvesting.

Thermoelectric materials could provide a clean and efficient way to solve the global energy and environmental crisis, thanks to their ability to generate electricity directly from untapped waste heat from various sources such as factories, computers, automobiles, and even human bodies.[1] The efficiency is defined by the dimensionless thermoelectric figure of merit $ZT = \sigma S^2 T/\kappa$, where σ, S, κ and T are the electrical conductivity, Seebeck coefficient, thermal conductivity, and absolute temperature, respectively. However, the development of highly efficient thermoelectric materials is still a great challenge because it requires decoupling of σ, S and κ, which are often unfavorably interdependent according to the Wiedemann–Franz law.[2] Intriguingly, recent studies have focused on decreasing κ through nanostructuring of the thermoelectric material to improve phonon scattering at the numerous grain boundaries.[1b,3] Unfortunately, while the phonon scattering is eminently enhanced by nanostructuring in, for example, quantum dots,[4] the electron scattering is also greatly increased, resulting in a concurrent reduction in σ and thus only a limited improvement in ZT. Herein we report a single-layer-based (SLB) composite fabricated from atomically thick single layers to optimize the thermoelectric parameters fully. This designed composite has several clear-cut advantages in increasing σ and S while simultaneously reducing κ (Scheme 1). Notably, both calculated and experimental results in our previous studies revealed that single layers and the corresponding SLB films can exhibit much increased densities of states (DOS) and carrier mobility (μ) compared with their bulk counterparts.[5] In this case, the single-layer configuration with atomic thickness could reasonably endow the SLB composite with increased σ along with an improvement in the thermoelectric energy harvesting.

Scheme 1. Exfoliation of 3D Bulk Materials into 2D Single Layers To Optimize the Thermoelectric Parameters

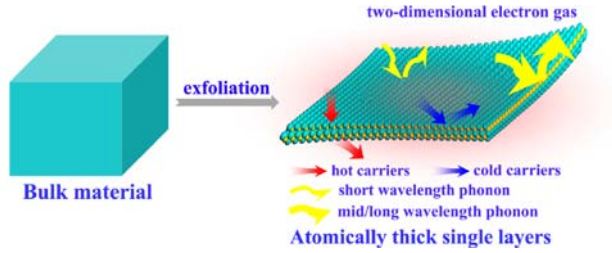

Moreover, according to the Hicks–Dresselhans model,[6] S^2 for quantum-well structures increases linearly with decreasing thickness because of the quantum confinement effect. Therefore, true atomic thickness would create a two-dimensional (2D) electron gas in the single layer, which would improve S for the SLB composite.[1a,8] Also, the potential barriers at the numerous interfaces and boundaries of the SLB composite would be expected to filter out low-energy carriers (cold carriers) and transmit high-energy carriers (hot carriers), thus leading to increased S.[3e] Furthermore, it is generally recognized that high σ is usually associated with large κ, which unfortunately offsets the former's effect on the thermoelectric performance. As is known, phonon characteristic lengths, including wavelengths and mean free paths, are usually much longer than those of electrons, enabling selective scattering of phonons rather than electrons. This has been demonstrated in some recent studies by Ren,

Received: October 16, 2012
Published: December 5, 2012

ACS Publications © 2012 American Chemical Society

dx.doi.org/10.1021/ja3102049 | J. Am. Chem. Soc. 2012, 134, 20294–20297

Chen, and Dresselhaus,[9] who clarified that the above contradiction can be resolved by suppressing phonon transport at the interfaces, boundaries, and defects, which reduces κ while maintaining σ. As such, the enormous grain boundaries and interfaces in the SLB composite could facilitate the scattering of mid/long-wavelength phonons, thus contributing to a reduction in κ with a minimal detrimental effect on the electrical properties. In addition, inorganic single layers with atomic thickness usually exhibit surface structural disorder,[5] allowing for efficient scattering of short-wavelength phonons, which decreases κ.[10] Therefore, further breakthroughs in the design and synthesis of novel atomically thick single layers having higher σ and S along with lower κ hold the key to the development of high-efficiency thermoelectric materials.

Inspired by the aforementioned concepts, we undertook the significant but challenging task of exploring the synthesis of atomically thick single layers in an effort to achieve high thermoelectric performance. For example, Bi_2Se_3[1b,11,12] possesses a layered structure in which the layers are held together by weak van der Waals interactions and each charge-neutral layer is composed of covalently bonded five-atom Se−Bi−Se−Bi−Se chains [Figure S1 in the Supporting Information (SI)]. In addition to its small band gap of 0.3 eV, the fascination with Bi_2Se_3 also comes from its unique 2D electron gas that covers the whole surface, thus contributing to metallic surface states. This suppresses the electron backscattering, ensuring a high μ of ~6000 $cm^2 V^{-1} s^{-1}$ and a Fermi velocity of $\sim 5 \times 10^5$ m/s.[7,13] As a result, the 2D electron gas and the phonon scattering at the grain boundaries and interfaces should enable a Bi_2Se_3 SLB composite to achieve improved σ and S as well as lower κ, thereby leading to an enhancement of ZT.

Herein we highlight the first successful synthesis of freestanding five-atom-thick Bi_2Se_3 single layers via a scalable intercalation/exfoliation strategy (Scheme S1 in the SI), which takes advantage of an intermediate precursor, Li-intercalated Bi_2Se_3 microplates (Figure S2B). Notably, the Tyndall effect of the colloidal suspension (Figure 1F inset) provides strong evidence for the homogeneous exfoliation of the Li-intercalated Bi_2Se_3 microplates (Figure S2B). Transmission electron microscopy (TEM) images of the exfoliated product reveal a clean, freestanding, flexible sheetlike morphology with a size up to 600 nm (Figure 1A and Figure S3), and its near transparency shows its ultrathin thickness. The corresponding high-resolution TEM (HRTEM) image and fast Fourier transform (FFT) pattern (Figure 1B,C) illustrate the single-crystalline nature of the exfoliated sheet with a [001] preferential orientation. Atomic force microscopy (AFM) images and the corresponding height profile and height distribution (Figure 1D,E and Figure S4) clearly show a smooth 2D sheet with a thickness of ca. 1 nm, fitting well with the height of 0.96 nm along the [001] direction for the single-layer Bi_2Se_3 slab (Figure S1). This gives solid direct evidence for the artificial synthesis of clean and freestanding five-atom-thick Bi_2Se_3 single layers. Since characterization of an individual single layer by X-ray diffraction (XRD) is difficult, a layer-by-layer (LbL) assembly strategy was used to fabricate a Bi_2Se_3 SLB film, whose XRD pattern was readily indexed to pure rhombohedral Bi_2Se_3 (JCPDS no. 89-2008) with a high degree of [001] orientation (Figure 1F). This confirmed that the Bi_2Se_3 single layers have a preferred [001] orientation, in accord with the HRTEM results (Figure 1B,C). Also, X-ray photoelectron spectra (Figure S5A−C) further confirmed the formation of pure Bi_2Se_3, while the corresponding down-shifted Raman bands could be ascribed to phonon softening with decreasing number of layers and hence indicated its ultrathin thickness (Figure S5D).[12f]

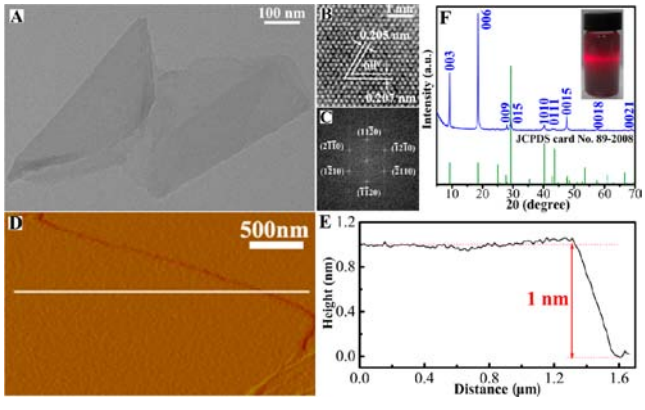

Figure 1. (A) TEM image, (B, C) HRTEM image and the corresponding FFT pattern, and (D, E) AFM image and the corresponding height profile for a freestanding Bi_2Se_3 single layer. (F) XRD pattern for a Bi_2Se_3 SLB film fabricated by LbL assembly. The inset shows the corresponding colloidal suspension, which was highly stable over 2 days and exhibited the typical Tyndall effect.

To study the local atomic arrangement and electronic structure of the five-atom-thick Bi_2Se_3 single layers, their Bi L_3-edge and Se K-edge synchrotron-radiation X-ray absorption fine structure (srXAFS) spectra were measured (Figure 2A).

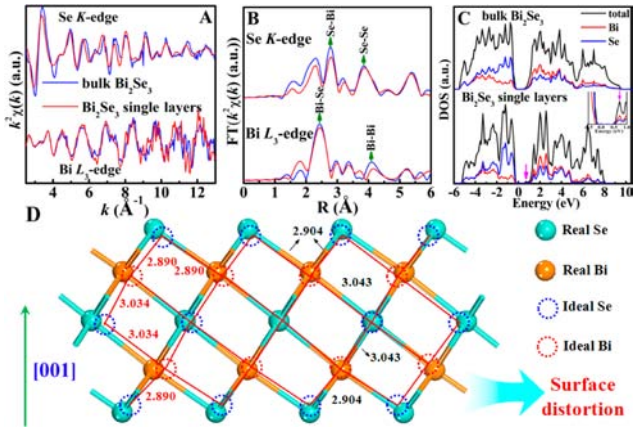

Figure 2. (A) Bi L_3-edge and Se K-edge extended XAFS oscillation functions $k^2\chi(k)$ and (B) the corresponding Fourier transforms for a Bi_2Se_3 single layer (red) and the bulk material (blue). (C) Calculated DOS. The inset shows an enlargement of the DOS for the single layer; the arrows denote the increased DOS at the CBM. (D) 2D structural model of a five-atom-thick Bi_2Se_3 single layer.

Compared with the bulk material, the Bi L_3-edge $k^2\chi(k)$ oscillation curve for the Bi_2Se_3 single layer displays a similar spectral shape along with a significant reduction in amplitude, indicating the difference in their local atomic arrangements. This was further verified by the corresponding Fourier transform (FT) $k^2\chi(k)$ functions in R space (Figure 2B). The FT curves for bulk Bi_2Se_3 possess peaks at 2.43 and 4.13 Å corresponding to the nearest Bi−Se and next-nearest Bi−Bi coordinations, respectively. In contrast, the peak intensities for the Bi_2Se_3 single layers are weakened, and the corresponding Bi−Bi peak position is shifted to larger R by 0.05 Å. Thus, the Bi L_3-edge spectra of the Bi_2Se_3 single layers qualitatively verify their distinct local atomic

dx.doi.org/10.1021/ja3102049 | J. Am. Chem. Soc. 2012, 134, 20294−20297

arrangement relative to the bulk material. This was further demonstrated by the Se K-edge FT spectra (Figure 2B), in which both the Se−Bi and Se−Se peaks for the Bi_2Se_3 single layer are shifted to larger R and noticeably less intense than those for the bulk material. To achieve the quantitative structural parameters around the Bi and Se atoms of the Bi_2Se_3 single layers and the bulk material, least-squares fits of the Bi L_3-edge and Se K-edge data were performed (Table S1 in the SI). Notably, the interatomic distances for the Bi−Se and Se−Bi coordinations in the Bi_2Se_3 single layers are slightly elongated and their degrees of disorder are much increased relative to the bulk material. The structural model of the Bi_2Se_3 single layer built according to the structural parameters in Table S1 is shown in Figure 2D, in which the distorted bond lengths are clearly labeled. Therefore, exfoliation of layered bulk Bi_2Se_3 into freestanding Bi_2Se_3 single layers does not induce an obvious change in the single-layer structure but does induce a noticeable intralayer structural distortion to minimize the surface energy and provide excellent structural stability. The surface disorder of an atomically thick Bi_2Se_3 single layer inevitably affects its electronic structure, so first-principles calculations were conducted using the atomic parameters obtained by srXAFS. The single layer was found to exhibit a much higher DOS at the conduction-band minimum (CBM) relative to the bulk material (Figure 2C). The enhanced DOS increases μ for the single layer, leading to its outstanding electrical properties.

As mentioned above, the coupling of σ, κ, and S unfortunately limits the efficiency of the materials and hence hinders their practical application.[14] Herein we highlight the successful synthesis of freestanding Bi_2Se_3 single layers and their subsequent fabrication into Bi_2Se_3 SLB composites through a cold compaction/sintering method (see the thermoelectric measurements in the SI), with efforts to optimize the thermoelectric parameters fully. The Bi_2Se_3 SLB composite exhibits a >2-fold increase in σ relative to the bulk material at 400 K (Figure 3A), demonstrating its excellent electrical properties. Moreover, κ of the SLB composite is much lower than that of the bulk material over the entire temperature range (Figure 3B). At 400 K, the SLB composite has $\kappa = 0.49$ W K^{-1} m^{-1}, which is ca. 2.5 times smaller than for the bulk material (1.2 W K^{-1} m^{-1}). Notably, the σ/κ ratio for the SLB composite is much higher than that for the bulk material over the whole temperature range, thanks to the increase in σ and concurrent decrease in κ (Figure 3D). Furthermore, $|S|$ for the SLB composite gradually increases from 90 μV/K at 300 K to 120.7 μV/K at 400 K, which is a factor of 1.2 greater than that of bulk material (98.5 μV/K) (Figure 3C). Meanwhile, the power factor (σS^2) of the SLB composite is much greater than that of the bulk material (Figure 3E), which could be a benefit of the simultaneously increased σ and S^2 values. Meanwhile, the positive T dependence of the power factor can be attributed to the coincident increases in σ and S^2 with increasing T. Also, ZT for the SLB composite is much higher than that for the bulk material over the whole temperature range (Figure 3F), and its features are fairly consistent with those of the T-dependent power factor (Figure 3E). In particular, the SLB composite exhibits $ZT = 0.35$ at 400 K, which is ca. 8 times larger than ZT for the bulk material and much higher than the previously reported values for pure Bi_2Se_3 nanostructures, suggesting the superiority of the atomically thick SLB structure.[1b,15]

It is notable that the calculated DOS at the conduction band edge is higher for the Bi_2Se_3 single layer than for the bulk material (Figure 2C). Thus, σ for the Bi_2Se_3 SLB composite is >2 times

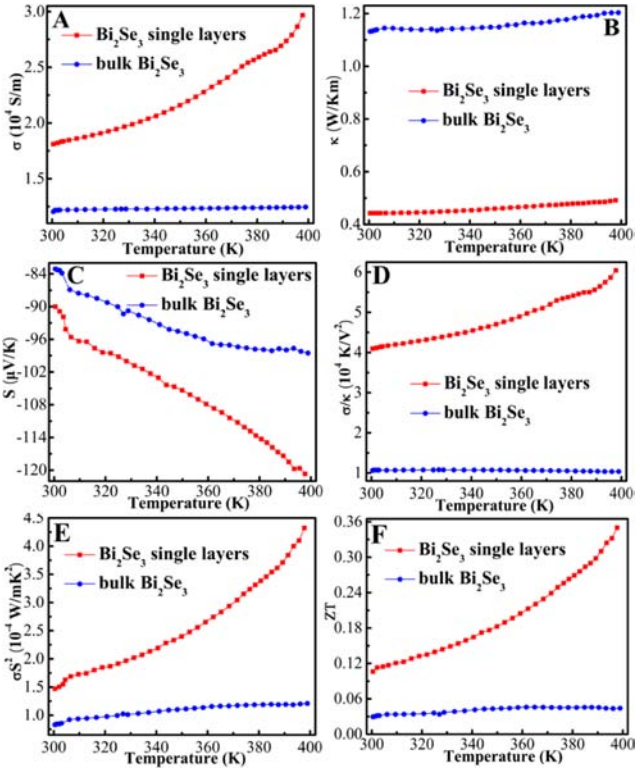

Figure 3. T dependence of (A) electrical conductivity (σ), (B) thermal conductivity (κ), (C) Seebeck coefficient (S), (D) σ/κ ratio, (E) power factor (σS^2), and (F) figure of merit (ZT) for the SLB composite and bulk Bi_2Se_3.

higher than that of the bulk material, indicating the fascinating superiority of the single-layer structure with atomic thickness. Also, the atomically ultrathin thickness and high degree of [001] orientation of the Bi_2Se_3 single layers further endow the SLB composite with unusual electronic properties, including 2D conducting channels and better grain-boundary connectivity,[5,11] as shown by its σ value (Figure 3A). In addition, it is noteworthy that nanostructuring could provide an efficient strategy to decrease κ through the enhanced phonon scattering at the numerous grain boundaries and interfaces.[1b,3c,8,9] In this regard, the five-atom-thick Bi_2Se_3 single layers endow the SLB composite with very high interface and boundary densities, which can effectively scatter mid/long-wavelength phonons and hence contribute to reducing κ. Meanwhile, the surface structural disorder revealed by srXAFS results in effective scattering of short-wavelength phonons, further decreasing κ.

Moreover, the semiclassical Mott−Jones formula[16] shows that S is inversely proportional to the carrier density (n) and can be estimated as $S \sim n^{-2/3}$.[17] As a result, one would expect S for the Bi_2Se_3 SLB composite to be much lower than that of the bulk material because of the much higher DOS in the Bi_2Se_3 single layers. However, the measured S values for the SLB composite and the bulk material disagree with that trend, suggesting that other factors such as potential-barrier scattering may play an important role in affecting n as well as the S.[8] It is noticeable that the potential barriers at the interfaces and grain boundaries can filter low-energy carriers, which are known to decrease S.[1b,3e,18] Accordingly, the eminently increased interface and boundary densities in the SLB composite facilitate the filtering of low-energy carriers and hence contribute to enhancing its S value. Meanwhile, the 2D electron gas covering the surface of each

dx.doi.org/10.1021/ja3102049 | J. Am. Chem. Soc. 2012, 134, 20294−20297

Bi_2Se_3 single layer further enhances S for the SLB composite because of the quantum confinement effect.[1a,5b,6,8,13] More importantly, according to the above discussion, it is known that the energy filtering by the interfacial barriers is an obvious hindrance only to the mobility of low-energy carriers.[1b,3e,18,19] Thus, μ for the SLB composite increases gradually with increasing T, thus leading to the positive T dependence of σ (Figure 3A).

In conclusion, a single-layer-based composite fabricated from atomically thick single layers has been developed to optimize the thermoelectric parameters fully. Clean, freestanding five-atom-thick Bi_2Se_3 single layers were artificially synthesized via a scalable intercalation/exfoliation strategy. Surface atomic elongation and structural disorder (as revealed by srXAFS and first-principles calculations) endow the Bi_2Se_3 single layer with excellent structural stability and much higher DOS at the conduction band edge, thus accounting for the 2 times higher σ. Also, the unique 2D electron gas and the "energy filtering" at the interfaces in the Bi_2Se_3 SLB composite increase the S value. Moreover, the numerous interfaces are effective at scattering mid/long-wavelength phonons, while the surface structural disorder facilitates short-wavelength phonon scattering, thus decreasing κ. As a result, the SLB composite achieved a ZT value of 0.35 at 400 K, which is ca. 8 times higher than that of the bulk material. The superior thermoelectric efficiency of the Bi_2Se_3 SLB composite is undoubtedly just one example showing the great promise of atomically thick SLB composites for future applications in tailoring the thermoelectric performance, thanks to their ability to overcome the disadvantages that occur in conventional nanostructuring, where optimizing one thermoelectric parameter often adversely affects others. The novel strategy developed here to optimize the coupled thermoelectric parameters should impact practical low/mid-temperature thermoelectric applications in various areas.

■ ASSOCIATED CONTENT

Supporting Information

Experimental procedures, computational details, and additional figures. This material is available free of charge via the Internet at http://pubs.acs.org.

■ AUTHOR INFORMATION

Corresponding Author

yxie@ustc.edu.cn; sqwei@ustc.edu.cn

Notes

The authors declare no competing financial interest.

■ ACKNOWLEDGMENTS

The authors thank Prof. Xianhui Chen and Dr. Xigang Luo of USTC for measurements of S and κ and the National Basic Research Program of China (2009CB939901) and the National Natural Science Foundation of China (11079004, 10979047, 90922016, 11135008, 21201157) for financial support.

■ REFERENCES

(1) (a) Ohta, H.; Kim, S.; Mune, Y.; Mizoguchi, T.; Nomura, K.; Ohta, S.; Nakanishi, Y.; Ikuhara, Y.; Hirano, M.; Hosono, H.; Koumoto, K. *Nat. Mater.* **2007**, *6*, 129. (b) Soni, A.; Yan, Y. Z.; Ligen, Y.; Aik, M.; Dresselhaus, M.; Xiong, Q. *Nano Lett.* **2012**, *12*, 1203.

(2) (a) Mehta, R. J.; Zhang, Y. L.; Karthik, C.; Singh, B.; Siegel, R. W.; Borca-Tasciuc, T.; Ramanath, G. *Nat. Mater.* **2012**, *11*, 233. (b) Fitsul, V. I. *Heavily Doped Semiconductors*; Plenum Press: New York, 1969.

(3) (a) Scheele, M.; Oeshler, N.; Veremchuk, L.; Reinsberg, K.; Kreuziger, A.; Kornowski, A.; Broekaert, J.; Klinke, C.; Weller, H. *ACS Nano* **2010**, *4*, 4283. (b) Teweldebrhan, D.; Goyal, V.; Rahman, M.; Balandin, A. A. *Appl. Phys. Lett.* **2010**, *96*, No. 053107. (c) Goyal, V.; Teweldebrhan, D.; Balandin, A. A. *Appl. Phys. Lett.* **2010**, *97*, No. 133117. (d) Zahid, F.; Lake, R. *Appl. Phys. Lett.* **2010**, *97*, No. 212102. (e) Son, J. S.; Choi, M. K.; Han, M. K.; Park, K.; Kim, J. Y.; Lim, S. J.; Oh, M.; Kuk, Y.; Park, C.; Kim, S. J.; Hyeon, T. *Nano Lett.* **2012**, *12*, 640. (f) Soni, A.; Shen, Y. Q.; Yin, M.; Zhao, Y. Y.; Yu, L. G.; Hu, X.; Dong, Z.; Khor, K. A.; Dresselhaus, M. S.; Xiong, Q. H. *Nano Lett.* **2012**, *12*, 4305. (g) Teweldebrhan, D.; Goyal, V.; Balandin, A. A. *Nano Lett.* **2010**, *10*, 1209.

(4) (a) Harman, T. C.; Taylor, P. J.; Walsh, M. P.; Laforge, B. E. *Science* **2002**, *297*, 2229. (b) Wang, R. Y.; Feser, J. P.; Lee, J. S.; Talapin, D. V.; Segalman, R.; Majumdar, A. *Nano Lett.* **2008**, *8*, 2283.

(5) (a) Sun, Y. F.; Sun, Z. H.; Gao, S.; Cheng, H.; Liu, Q. H.; Piao, J.; Yao, T.; Wu, C. Z.; Hu, S. L.; Wei, S. Q.; Xie, Y. *Nat. Commun.* **2012**, *3*, 1057. (b) Sun, Y. F.; Cheng, H.; Gao, S.; Sun, Z. H.; Liu, Q. H.; Liu, Q.; Lei, F. C.; Yao, T.; He, J. F.; Wei, S. Q.; Xie, Y. *Angew. Chem., Int. Ed.* **2012**, *51*, 8727.

(6) Hicks, L. D.; Dresselhaus, M. S. *Phys. Rev. B* **1993**, *47*, 12727.

(7) Peng, H. L.; Dang, W. H.; Cao, J.; Chen, Y. L.; Wu, D.; Zheng, W. S.; Li, H.; Shen, Z. X.; Liu, Z. F. *Nat. Chem.* **2012**, *4*, 281.

(8) Takei, K.; Madsen, M.; Fang, H.; Kapadia, R.; Chuang, S.; Kim, H. S.; Liu, C.; Plis, E.; Nah, J.; Krishna, S.; Chueh, Y.; Guo, J.; Javey, A. *Nano Lett.* **2012**, *12*, 2060.

(9) (a) Minnich, A. J.; Dresselhaus, M. S.; Ren, Z. F.; Chen, G. *Energy Environ. Sci.* **2009**, *2*, 466. (b) Zebarjadi, M.; Esfarjani, K.; Dresselhaus, M. S.; Ren, Z. F.; Chen, G. *Energy Environ. Sci.* **2012**, *5*, 5147. (c) Liu, W. S.; Yan, X.; Chen, G.; Ren, Z. F. *Nano Energy* **2012**, *1*, 42. (d) Poudel, B.; Hao, Q.; Ma, Y.; Lan, Y. C.; Minnich, A.; Yu, B.; Yan, X.; Wang, D. Z.; Muto, A.; Vashaee, D.; Chen, X. Y.; Liu, J. M.; Dresselhaus, M. S.; Chen, G.; Ren, Z. F. *Science* **2008**, *320*, 634. (e) Yan, Y.; Poudel, B.; Ma, Y.; Liu, W. S.; Joshi, G.; Wang, H.; Lan, Y. C.; Wang, D. Z.; Chen, G.; Ren, Z. F. *Nano Lett.* **2010**, *10*, 3373.

(10) (a) Chiritescu, C.; Cahill, D. G.; Nguyen, N.; Johnson, D.; Bodapati, A.; Keblinski, P.; Zschack, P. *Science* **2007**, *315*, 351. (b) Snyder, G. J.; Christensen, M.; Nishibori, E.; Caillat, T.; Iversen, B. B. *Nat. Mater.* **2004**, *3*, 458.

(11) Hossain, M. Z.; Rumyantsev, S. L.; Shahil, K. M. F.; Teweldebrhan, D.; Shur, M.; Balandin, A. A. *ACS Nano* **2011**, *5*, 2657.

(12) (a) Li, H.; Cao, J.; Zheng, W. S.; Chen, Y. L.; Wu, D.; Dang, W. H.; Wang, K.; Peng, H. L.; Liu, Z. F. *J. Am. Chem. Soc.* **2012**, *134*, 6132. (b) Min, Y.; Moon, G. D.; Kim, B. S.; Lim, B.; Kim, J. S.; Kang, C. Y.; Jeong, U. *J. Am. Chem. Soc.* **2012**, *134*, 2872. (c) Shahil, K. M. F.; Hossain, M. Z.; Goyal, V.; Balandin, A. A. *J. Appl. Phys.* **2012**, *111*, No. 054305. (d) Koski, K. J.; Cha, J. J.; Reed, B. W.; Wessells, C. D.; Kong, D. S.; Cui, Y. *J. Am. Chem. Soc.* **2012**, *134*, 7584. (e) Hong, S. S.; Kundhikanjana, W.; Cha, J. J.; Lai, K.; Kong, D. S.; Meister, S.; Kelly, M. A.; Shen, Z. X.; Cui, Y. *Nano Lett.* **2010**, *10*, 3118. (f) Zhang, J.; Peng, Z. P.; Soni, A.; Zhao, Y. Y.; Xiong, Y.; Peng, B.; Wang, J. B.; Dresselhaus, M. S.; Xiong, Q. H. *Nano Lett.* **2011**, *11*, 2407.

(13) (a) Zhang, H.; Liu, C. X.; Qi, X. L.; Dai, X.; Fang, Z.; Zhang, S. C. *Nat. Phys.* **2009**, *5*, 438. (b) Kou, X. F.; He, L.; Xiu, F. X.; Lang, M. R.; Liao, Z. M.; Wang, Y.; Fedorov, A. V.; Yu, X. X.; Tang, J. S.; Huang, G.; Jiang, X. W.; Zhu, J. F.; Zou, J.; Wang, K. L. *Appl. Phys. Lett.* **2011**, *98*, No. 242102.

(14) Liu, H. L.; Shi, X.; Xu, F. F.; Zhang, L. L.; Zhang, W. Q.; Chen, L. D.; Li, Q.; Uher, C.; Day, T.; Snyder, G. J. *Nat. Mater.* **2012**, *11*, 422.

(15) Kadel, K.; Kumari, L.; Li, W. Z.; Huang, J. Y.; Provencio, P. P. *Nanoscale Res. Lett.* **2011**, *6*, 57.

(16) (a) Jonson, M.; Mahan, G. D. *Phys. Rev. B* **1980**, *21*, 4223. (b) Schiller, W.; Richter, J. *Phys. Status Solidi B* **1982**, *114*, 151.

(17) Snyder, G. J.; Toberer, E. S. *Nat. Mater.* **2008**, *7*, 105.

(18) Dresselhaus, M. S. *Adv. Mater.* **2007**, *19*, 1043.

(19) Zhang, Y. C.; Snedaker, M. L.; Birkel, C. S.; Mubeen, S.; Ji, X. L.; Shi, Y. F.; Liu, D.; Liu, X. N.; Moskovits, M.; Stucky, G. D. *Nano Lett.* **2012**, *12*, 1075.